

Review

# Recent Advances in Atmospheric Chemistry of Mercury

Lin Si <sup>1,\*</sup> and Parisa A. Ariya <sup>2,\*</sup> 

<sup>1</sup> Department of Chemistry, Auburn University at Montgomery, 7400 East Dr., Montgomery, AL 36117, USA

<sup>2</sup> Department of Chemistry & Department of Atmospheric and Oceanic Sciences, McGill University, 801 Sherbrooke St. W., Montreal, QC H3A 2K6, Canada

\* Correspondence: lsi1@aum.edu (L.S.); parisa.ariya@mcgill.ca (P.A.A.)

Received: 20 January 2018; Accepted: 15 February 2018; Published: 21 February 2018



**Abstract:** Mercury is one of the most toxic metals and has global importance due to the biomagnification and bioaccumulation of organomercury via the aquatic food web. The physical and chemical transformations of various mercury species in the atmosphere strongly influence their composition, phase, transport characteristics and deposition rate to the ground. Modeling efforts to evaluate the mercury cycling in the environment require an accurate understanding of atmospheric mercury chemistry. We focus this article on recent studies (since 2015) on improving our understanding of the atmospheric chemistry of mercury. We discuss recent advances in (i) determining the dominant atmospheric oxidant of elemental mercury ( $\text{Hg}^0$ ); (ii) understanding the oxidation reactions of  $\text{Hg}^0$  by halogen atoms and by nitrate radical ( $\text{NO}_3$ ); (iii) the aqueous reduction of oxidized mercury compounds ( $\text{Hg}^{\text{II}}$ ); and (iv) the heterogeneous reactions of Hg on atmospherically-relevant surfaces. The need for future research to improve understanding of the fate and transformation of mercury in the atmosphere is also discussed.

**Keywords:** mercury; atmospheric chemistry; recent progress; future research needs

## 1. Introduction

Mercury (Hg) is one of the most toxic metals present globally in the environment [1]. Due to the rather long lifetime of atmospheric mercury, once mercury compounds are released into the atmosphere, they can be transported around the globe. As such, they not only have local impacts but also regional and global implications [2,3].

Hg is a Group IIB transition metal with an atomic number of 80 and a closed shell electronic configuration ( $5d^{10} 6s^2$ ). Elemental mercury ( $\text{Hg}^0$ ) is the only liquid metal at room temperature and pressure. Mercury has been widely used in electrochemistry, in optical spectroscopy, in liquid mirror telescopes and also in medicine. However, tragic outbreaks of mercury-induced diseases have occurred in many areas of the world over the years, particularly in Japan and Iraq [4]. Mercury toxicity depends on its chemical species, with methylmercury being highly toxic. Humans and wildlife are exposed to mercury mainly through fish consumption. Exposure to mercury can damage the human nervous system, cause cardiovascular diseases in adults, impede cognitive development in children, as well as affect the reproduction of fish, mammals and birds ([5] and references therein).

Atmospheric deposition has been identified as a significant pathway for Hg transport into the aquatic and soil environment. It has been estimated that 5500–8900 tons of mercury are emitted per year into the atmosphere, with three major natural, anthropogenic and re-emitted sources [2]. Natural sources of Hg emission include volcanoes, soils, forests, natural waters, and the largest anthropogenic source of Hg emission is coal burning in coal fueled power plants [6]. Previously-deposited mercury can be re-emitted to the atmosphere through a series of physical, chemical and biological transformations

in the environment [7,8]. Large uncertainties remain in existing emission inventories, particularly for natural and re-emission sources [9].

Figure 1a illustrates a simplified picture of mercury transformations in the environment, particularly on various environmental surfaces, and Figure 1b focuses on the atmospheric chemistry of mercury. In the atmospheric environment, mercury presents predominantly in oxidation states of 0 and +2 [10]. Atmospheric mercury exists in the gas phase, in atmospheric droplets, or in the particulate phase. Mercury speciation significantly affects the rates of dry and wet deposition and subsequently, the atmospheric lifetimes of different Hg species [11]. For example, gaseous elemental mercury ( $\text{Hg}^0$ ) has been estimated to have an atmospheric lifetime of about one year [4,12], which render it subject to long-range transportation across the globe. However, atmospheric oxidation of  $\text{Hg}^0$  to  $\text{HgBr}_2$  will make mercury more subject to deposition, due to the low solubility of  $\text{Hg}^0$  and high solubility of  $\text{HgBr}_2$  in atmospheric droplets. The deposition of oxidized mercury can make Hg potentially become available to biota [4]. Field studies have demonstrated the fast oxidation of  $\text{Hg}^0$  to  $\text{Hg}^{\text{II}}$  in the Arctic and Antarctic regions after polar sunrise, a phenomenon known as Arctic mercury depletion events (AMDEs). The explanation of this fascinating phenomenon will rely on fully understanding the redox reactions of atmospheric Hg [13]. On the other hand, atmospheric Hg models are essential tools for interpreting field observations and evaluating pollution control policies [10]. The further advancement of atmospheric Hg modeling depends on accurate kinetic data on the oxidation and reduction reactions of various mercury species in the atmosphere. However, many important processes involved in the transformation and deposition of atmospheric Hg are yet to be identified or quantified [14]. Global modeling studies also suggest that large uncertainties exist in our current knowledge of the global cycling of mercury [15].

The chemistry of atmospheric mercury was previously reviewed in detail by Lin and Pehkonen [16], Ariya et al. [17], Subir et al. [18], Lin et al. [14] and Ariya et al. [4]. Several excellent contributions have been made to our understanding in this area since 2015. The objective of this article is to discuss the current understanding of atmospheric mercury chemistry, with more focus on recent laboratory, theoretical, field and model studies since 2015 on the interconverting reactions between  $\text{Hg}^0$  and  $\text{Hg}^{\text{II}}$ . Finally, future research is recommended in order to further advance our knowledge of the dynamic transformations of atmospheric mercury.

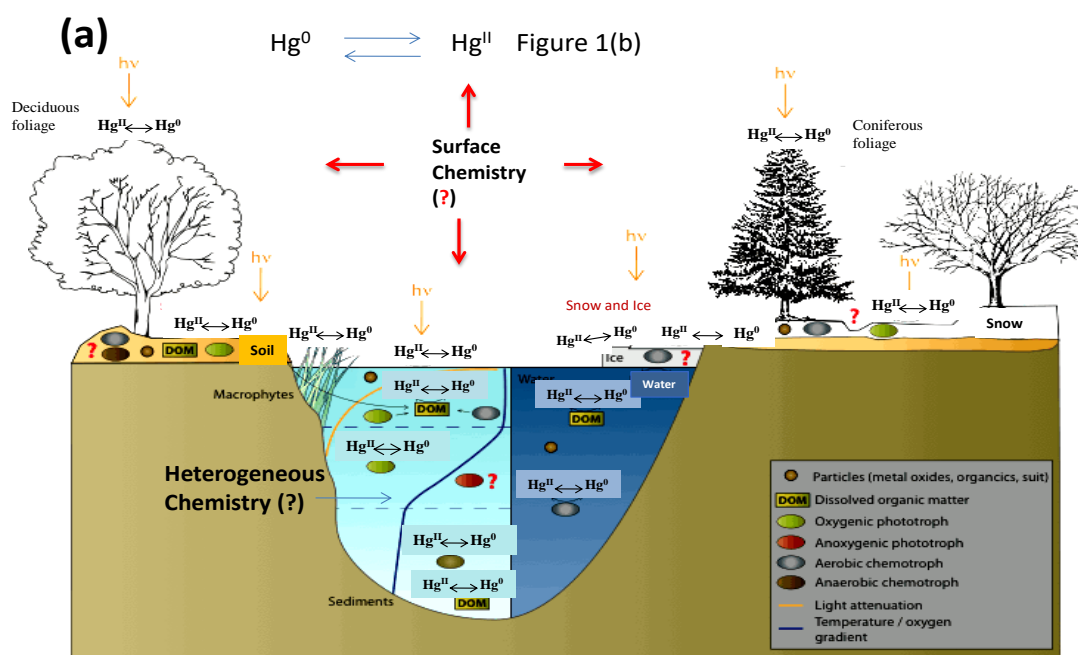
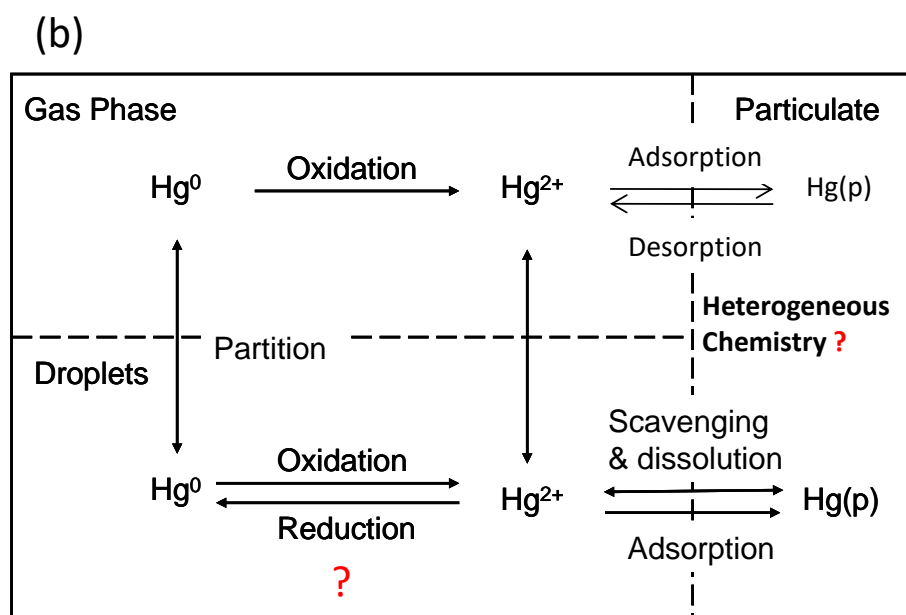


Figure 1. Cont.



**Figure 1.** (a) Mercury transformations in the environment; (b) Atmospheric chemistry of mercury. Adapted and modified from [3]. The question mark (?) indicates some major knowledge gaps in Hg cycling in the environment.

## 2. Chemical Redox Pathways in the Gas Phase

The oxidation of  $\text{Hg}^0$  is a very crucial step for the removal of Hg from the atmosphere. Understanding the oxidation reactions of  $\text{Hg}^0$  is important for estimating the atmospheric lifetime of mercury. To date, the proposed oxidation pathways of  $\text{Hg}^0$  in the gas phase include the oxidation of  $\text{Hg}^0$  by  $\text{O}_3$ ,  $\text{H}_2\text{O}_2$ , OH radical,  $\text{NO}_3$  radical and by various halogen species [14]. Table 1 lists the gas-phase oxidation reactions of  $\text{Hg}^0$  and the reported rate coefficients. As shown in Figure 2 in Subir et al. [18], large variations exist in the current reported rate constants of gas-phase oxidation reactions of Hg. Here we discuss recent advances in the understanding of the oxidation of  $\text{Hg}^0$  by halogen atoms and  $\text{NO}_3$  radicals, as well as determining the major oxidant(s) in the atmosphere.

**Table 1.** Current accumulated knowledge on the chemical redox pathways of Hg in the gas phase.

Gas Phase Reaction	Diluent Gas <sup>a</sup> (T = 298 K)	Rate Coefficient <sup>b</sup> (cm <sup>3</sup> molec <sup>-1</sup> s <sup>-1</sup> )	References
$Hg^0 + Br \rightarrow HgBr$	Air, N <sub>2</sub> , 1 atm	$(3.2 \pm 0.3) \times 10^{-12}$	[19]
	Air, NO, 1 atm	$9 \times 10^{-13}$	[20]
	N/A, 1 atm <sup>c</sup>	$1.01 \times 10^{-12} \exp(209.03/T)$	[3]
	N/A, 1 atm	$2.07 \times 10^{-12}$	
	N/A (180–400 K)	$1.1 \times 10^{-12} (T/298K)^{-2.37}$	[21]
	N/A, 1 atm	$1.1 \times 10^{-12}$	
	N <sub>2</sub> , 1 atm (243–298 K)	$(1.46 \pm 0.34) \times 10^{-32} \times (T/298)^{-(1.86 \pm 1.49)} \text{ cm}^6/\text{molec}^2/\text{s}$	[22]
	N <sub>2</sub> , 1 atm	$(3.6 \pm 0.9) \times 10^{-13}$	
$HgBr + M \rightarrow BrHgM$ M = NO <sub>2</sub> or HO <sub>2</sub>	Ar, 1 atm (260 K) <sup>c</sup>	$1.2 \times 10^{-12}$	[23]
	Air, 1 atm	$(1.6 \pm 0.8) \times 10^{-12}$	[24]
$HgBr + Br \rightarrow HgBr_2$	N/A (220–320 K)	$k ([M], T)^d$	[25]
	CF <sub>3</sub> Br, 0.26 atm (397 K)	$7 \times 10^{-17}$	[26]
	N/A, 1 atm (180–400 K)	$2.5 \times 10^{-10} (T/298K)^{-0.57}$	[21]
$Hg^0 + Cl \rightarrow HgCl$	N/A, 1 atm	$2.5 \times 10^{-10}$	
	Ar, 0.93 atm (383–443 K)	$(3.2 \pm 1.7) \times 10^{-11}$	[27]
	Air, NO, 1 atm	$6.4 \times 10^{-11}$	[20]
	Air, N <sub>2</sub> , 1 atm	$(1.0 \pm 0.2) \times 10^{-11}$	[19]
	N/A, 1 atm <sup>c</sup>	$1.38 \times 10^{-12} \exp(208.02/T)$	[3]
	N/A, 1 atm	$2.81 \times 10^{-12}$	
	N <sub>2</sub> (243–298 K)	$(2.2 \pm 0.5) \times 10^{-32} \times \exp [(680 \pm 400)(1/T - 1/298)] \text{ cm}^6/\text{molec}^2/\text{s}$	[28]
	N <sub>2</sub> , 1 atm	$5.4 \times 10^{-13}$	
$Hg^0 + O_3 \rightarrow HgO_{(s)} + O_2$	N <sub>2</sub> , 1 atm	$1.2 \times 10^{-10}$	[29]
	Air, 1 atm	$(1.8 \pm 0.5) \times 10^{-11}$	[24]
	N/A, 1 atm (293 K)	$4.2 \times 10^{-19}$	[30,31]
	N/A, 1 atm (293 K)	$4.9 \times 10^{-18}$	[31,32]
	Air, 1 atm (293 K)	$1.7 \times 10^{-18}$	[33]
	N <sub>2</sub> /O <sub>2</sub> , 1 atm (293 K)	$(3 \pm 2) \times 10^{-20}$	[34]
	N <sub>2</sub> , 1 atm	$(7.5 \pm 0.9) \times 10^{-19}$	[35]
	Air, 1 atm	$(6.4 \pm 2.3) \times 10^{-19}$	[36]
	N <sub>2</sub> , 1 atm	$(6.2 \pm 1.1) \times 10^{-19}$	[37]
Air, 1 atm	$(7.4 \pm 0.5) \times 10^{-19}$	[38]	

Table 1. Cont.

Gas Phase Reaction	Diluent Gas <sup>a</sup> ( <i>T</i> = 298 K)	Rate Coefficient <sup>b</sup> (cm <sup>3</sup> molec <sup>-1</sup> s <sup>-1</sup> )	References
$Hg^0 + OH \rightarrow HgOH$	Air, 1 atm	$(8.7 \pm 2.8) \times 10^{-14}$	[39]
	N/A, 1 atm (343 K)	$(1.6 \pm 0.2) \times 10^{-11}$	[40]
	Air, 1 atm	$< 1.2 \times 10^{-13}$	[41]
$HgOH + O_2 \rightarrow HgO_{(s)} + OH$	N/A, 1 atm (180–400 K)	$3.2 \times 10^{-13} (T/298K)^{-3.06}$	[21]
	N/A, 1 atm	$3.2 \times 10^{-13}$	
	Air/N <sub>2</sub> , 1 atm	$(9.0 \pm 1.3) \times 10^{-14}$	[42]
$Hg^0 + F \rightarrow HgF$	N/A, 1 atm <sup>c</sup>	$9.2 \times 10^{-13} \exp(206.81/T)$	[3]
	N/A, 1 atm	$1.86 \times 10^{-12}$	
$Hg^0 + I \rightarrow HgI$	N/A, 1 atm (180–400 K)	$4.0 \times 10^{-13} (T/298 K)^{-2.38}$	[21]
	N/A, 1 atm	$4.0 \times 10^{-13}$	
$Hg^0 + F_2 \rightarrow Hg^{2+} + Products$	Air, 1 atm	$(1.8 \pm 0.4) \times 10^{-15}$	[36]
	N <sub>2</sub> , 1 atm	$\leq (1.27 \pm 0.58) \times 10^{-19}$	[43]
$Hg^0 + Cl_2 \rightarrow HgCl_2$	Air, N <sub>2</sub> , 1 atm	$(2.6 \pm 0.2) \times 10^{-18}$	[19]
	Air, 1 atm	$(2.5 \pm 0.9) \times 10^{-18}$	[36]
	N <sub>2</sub> , 1 atm	$4.3 \times 10^{-15}$	[29]
$Hg^0 + Br_2 \rightarrow HgBr_2$	Air, N <sub>2</sub> , 1 atm	$< (0.9 \pm 0.2) \times 10^{-16}$	[19]
$Hg^0 + ClO \rightarrow HgClO$	N <sub>2</sub> , 1 atm	$1.1 \times 10^{-11}$	[29]
$Hg^0 + BrO \rightarrow HgBrO$	Air, NO, 1 atm	$(3.0\text{--}6.4) \times 10^{-14}$	[20]
	N <sub>2</sub> , 1 atm	$(1\text{--}100) \times 10^{-15}$	[44]
$Hg^0 + NO_3 \rightarrow HgO + NO_2$	N <sub>2</sub> , $(5\text{--}10) \times 10^{-3}$ atm (294 K)	$< 4 \times 10^{-15}$	[39]
	Air, 1 atm	$< 7 \times 10^{-15}$	[36]
$Hg^0 + H_2O_2 \rightarrow HgO + H_2O$	N/A, 1 atm	$< 4.1 \times 10^{-16}$	[45]
	N <sub>2</sub> , N/A (293 K)	$< 8.5 \times 10^{-19}$	[46]

<sup>a</sup> *T* = 298 K, unless otherwise stated; <sup>b</sup> The unit is cm<sup>3</sup> molec<sup>-1</sup> s<sup>-1</sup> unless otherwise stated; <sup>c</sup> Temperature range is unknown. <sup>d</sup>  $k([M], T) = \left( \frac{k^0(T)[M]}{1 + \frac{k^0(T)[M]}{k^\infty(T)}} \right) 0.6^{\left( \frac{1}{1 + \log\left( \frac{k^0(T)[M]}{k^\infty(T)} \right)^2} \right)}$  where  $k^0(T)$  and  $k^\infty(T)$  values are tabulated in [25].

### 2.1. Br-Initiated Oxidation of $\text{Hg}^0$

The oxidation of  $\text{Hg}^0$  by Br occurs via a two-step process with  $\text{HgBr}$  as the intermediate. Previous quantum calculations by Dibble et al. [47] demonstrated that  $\text{BrHg}$  could react with the abundant radicals in the atmosphere to form stable  $\text{BrHgY}$  compounds where Y is  $\text{NO}_2$ ,  $\text{HO}_2$ ,  $\text{ClO}$ , or  $\text{BrO}$ . Previous laboratory studies reported apparent rate coefficients in the range of  $(3.6 \pm 0.9) \times 10^{-13}$  to  $(3.2 \pm 0.3) \times 10^{-12} \text{ cm}^3 \text{ molec}^{-1} \text{ s}^{-1}$ , at 1 atm and 298 K [19,20,22]. Theoretical studies estimated the rate constants to be from  $9.8 \times 10^{-13}$  to  $2.1 \times 10^{-12} \text{ cm}^3 \text{ molec}^{-1} \text{ s}^{-1}$ , at 1 atm and 298 K [3,21,23]. Theoretical and experimental rate constants for mercury oxidation by Br and Cl atoms at 298 K have previously been compared in detail in Table A.2 by Subir et al. [18].

The first kinetic study of the reactions of  $\text{BrHg}$  with  $\text{NO}_2$  and  $\text{HO}_2$  was recently reported by Jiao and Dibble [25], using computational chemistry. Quantum calculations were performed to obtain the rate constants and product yields for the oxidation reactions of  $\text{BrHg}$  with  $\text{NO}_2$  and  $\text{HO}_2$ . The rate constant for the oxidation of  $\text{HgBr}$  by  $\text{NO}_2$  was larger than that for the oxidation of  $\text{HgBr}$  by  $\text{HO}_2$  ( $T = 200\text{--}320 \text{ K}$ ). The fate of  $\text{HgBr}$  relied more on the concentration ratio of  $[\text{NO}_2]/[\text{HO}_2]$  in the atmosphere than the ratio of their oxidation rate constants. While the addition reaction dominated the reaction of  $\text{HgBr}$  by  $\text{HO}_2$ , the addition of  $\text{HgBr}$  by  $\text{NO}_2$  was competed by a reduction reaction to form  $\text{Hg} + \text{BrNO}_2$  (up to 18% of the oxidation). The reaction product of the oxidation of  $\text{HgBr}$  by  $\text{NO}_2$  was computed to be syn- $\text{BrHgONO}$  under atmospheric conditions. Because no experimental studies on the reaction of  $\text{HgBr}$  of  $\text{NO}_2$  and  $\text{HO}_2$  have been previously reported in the literature, the rate constants computed in this study are significant for future model and laboratory studies [25].

Sun et al. [24] used a relative rate technique with ethane and propene as references and determined the rate coefficients for  $\text{Hg}^0 + \text{Br}\bullet$  reactions to be  $(1.6 \pm 0.8) \times 10^{-12} \text{ cm}^3 \text{ molec}^{-1} \text{ s}^{-1}$ , at 100 kPa and  $298 \pm 3 \text{ K}$ . The determined rate coefficient was in the midst of previously reported rate constants. Measurements using a scanning mobility particle sizer by Sun et al. [24] also showed that Hg products largely existed as wall deposits in agreement with the previous product analysis by Ariya et al. [19]. It has been suggested that the presence of aerosols in the Aitken mode during the oxidation reaction may be initiated by the vapor nucleation of mercury-containing products.

### 2.2. Cl-Initiated Oxidation of $\text{Hg}^0$

Similar to  $\text{Hg}^0$ -Br oxidation, the oxidation of  $\text{Hg}^0$  by atomic Cl was believed to occur via a two-step chlorination process with  $\text{HgCl}$  as the intermediate [19,24,28]. Theoretical calculations indicated that after the initializing step to form the  $\text{HgCl}$  intermediate, the secondary oxidation of  $\text{HgCl}$  could be carried out by  $\text{NO}_2$ ,  $\text{HO}_2$ ,  $\text{ClO}$ , or  $\text{BrO}$  [47]. Recently, Sun et al. [24] determined the rate coefficients using a relative rate technique with ethane and 2-chloro-propane as references. The rate coefficient for the  $\text{Hg}^0 + \text{Cl}\bullet$  reaction was reported to be  $(1.8 \pm 0.5) \times 10^{-11} \text{ cm}^3 \text{ molecule}^{-1} \text{ s}^{-1}$ , at 100 kPa and  $298 \pm 3 \text{ K}$ , which was in agreement with three earlier laboratory studies by Horne et al. [27], Spicer et al. [20] and Ariya et al. [19] ( $1.0\text{--}6.4 \times 10^{-11} \text{ cm}^3 \text{ molecule}^{-1} \text{ s}^{-1}$ ). However, the reported rate coefficient was about two orders of magnitude larger than that determined by Donohoue et al. [28] ( $5.4 \times 10^{-13} \text{ cm}^3 \text{ molecule}^{-1} \text{ s}^{-1}$ ) and one order of magnitude smaller than that determined by Byun et al. [29] ( $1.2 \times 10^{-10} \text{ cm}^3 \text{ molecule}^{-1} \text{ s}^{-1}$ ). The determined rate constant was one order of magnitude higher than the only theoretical estimation by Khalizov et al. [2] ( $2.81 \times 10^{-12} \text{ cm}^3 \text{ molecule}^{-1} \text{ s}^{-1}$ ).

More studies are needed to reduce the uncertainties in the kinetic estimate of the oxidation reactions of atmospheric Hg. To render it more complex, as the existing reactions show the importance of surfaces in catalysis and heterogeneous reactions [4,48], further studies on atmospherically-relevant surfaces are recommended.

### 2.3. Oxidation of $\text{Hg}^0$ by $\text{NO}_3$

The experimentally-determined rate constant for the oxidation of  $\text{Hg}^0$  by  $\text{NO}_3$  has been previously reported to be  $<4 \times 10^{-15} \text{ cm}^3 \text{ molecule}^{-1} \text{ s}^{-1}$  by Sommar et al. [39] and  $<7 \times 10^{-15} \text{ cm}^3 \text{ molecule}^{-1} \text{ s}^{-1}$  by Sumner et al. [36] at 1 atm and 298 K. However, based on the new HgO thermochemistry, Hynes et al. estimated this reaction to be highly endothermic and, thus, suggested that this oxidation pathway is not viable in the atmosphere [14,49]. Furthermore, theoretical calculations by Dibble et al. [47] suggest that  $\text{NO}_3$  do not form strong bonds with  $\text{Hg}^0$  and therefore is unlikely to initiate gas-phase  $\text{Hg}^0$  oxidation reactions.

A recent study by Peleg et al. [50] provided field evidence of the possible participation of nitrate radicals ( $\text{NO}_3$ ) in the nighttime oxidation of  $\text{Hg}^0$  in the atmosphere. In their study, the role of  $\text{NO}_3$  in the nighttime oxidation of  $\text{Hg}^0$  in the atmosphere was evaluated by measuring the concentrations of  $\text{NO}_3$ ,  $\text{Hg}^0$  and  $\text{Hg}^{\text{II}}$  continuously during a six-week period in the urban air shed of Jerusalem, Israel during the summer of 2012. The  $R^2$  average of 0.47 indicated a strong correlation between nighttime [ $\text{Hg}^{\text{II}}$ ] and [ $\text{NO}_3$ ], while correlations of nighttime [ $\text{Hg}^{\text{II}}$ ] with other environmental variables were either weak or absent. Detailed analyses implied that  $\text{NO}_3$  radicals may be involved in the  $\text{Hg}^0$  oxidation reaction in the atmosphere. Previous theoretical calculations suggested that  $\text{NO}_3$  may be unlikely to initiate  $\text{Hg}^0$  oxidation [47,49]; therefore,  $\text{NO}_3$  may be involved in the secondary oxidation reaction of unstable  $\text{Hg}^{\text{I}}$  species [50]. More laboratory and theoretical studies are required to assess the role of  $\text{NO}_3$  in secondary reactions of  $\text{Hg}^0$  oxidation in the real atmosphere, including on atmospherically-relevant surfaces.

### 2.4. Dominant Gaseous Oxidant for $\text{Hg}^0$ : $\text{O}_3/\text{OH}$ , Br or Others?

Previous studies have assumed  $\text{O}_3$  and OH to be the major  $\text{Hg}^0$  oxidants in the atmosphere [51–56]. Despite theoretical doubts concerning the thermal stability of gaseous  $\text{HgOH}$  and  $\text{HgO}$  products, many modeling results using  $\text{O}_3/\text{OH}$  as the main atmospheric Hg oxidants showed good agreement with the observed  $\text{Hg}^0$  concentration and wet deposition flux. However, more complex atmospheric Hg oxidation reactions, particularly heterogeneous reactions involving  $\text{O}_3$  and OH, have been implied in recent studies ([57] and references therein).

Atomic bromine (Br) has been suggested to be the dominant oxidant of  $\text{Hg}^0$  in the marine boundary layer and in the Arctic [58–60]. A previous model study by Holmes et al. [61] implied that Br could be the major oxidant of  $\text{Hg}^0$  in the global atmosphere. The existence of BrO radical has been reported in the upper troposphere [62,63] and over the southeastern US [5,64]. Due to the rapid exchange between Br and BrO radicals [65] and the much slower oxidation rate of  $\text{Hg}^0$  by BrO [18] the field observations of BrO seem to support the dominant oxidation of  $\text{Hg}^0$  by Br in the atmosphere. Shah et al. [5] found that sensitivity simulations using the GEOS-Chem chemical transport model by either increasing Br concentrations, or using a faster rate constant for the oxidation reaction of  $\text{Hg}^0$  by Br, resulted in a better agreement between the modeled results and the aircraft observations. Yet, consistent BrO measurements do not exist in the lower troposphere where humans and biota exist. Moreover, note that the majority of chemical compounds are more concentrated and diversified in the boundary layer, which leads to much more complexity in chemistry, physics and biology due to various interfacial processes. The field studies by Gust and co-workers during the last decades also suggested that  $\text{Hg}^0$  may be oxidized not just by Br or BrO, but also by various oxidants in the atmosphere. The composition of oxidized mercury showed that  $\text{Hg}^0$  is subject to oxidation processes with various oxidants and not necessarily Br. The assumption of using Br as a universal global oxidant for atmospheric Hg may need further evaluation [66].

The most recent modeling studies indicated more complex Hg chemistry in the atmosphere, and multiple oxidants may be significant under various atmospheric conditions. Ye et al. [67] developed a box model including up-to-date atmospheric Hg chemistry and used it to study the oxidation of  $\text{Hg}^0$  at three different locations in the northeastern United States. The simulated diurnal cycles of  $\text{Hg}^{\text{II}}$  agreed well with the observations. Model results showed that  $\text{Hg}^0$  oxidation was dominated by  $\text{O}_3$  and OH at the coastal and inland sites during the day and  $\text{Hg}^0$  oxidation initiated by  $\text{H}_2\text{O}_2$

was significant at the inland site during the night. In the marine boundary layer (MBL), the model simulations indicated that Br/BrO were the major oxidants of  $\text{Hg}^0$  at midday while  $\text{O}_3$  became the dominant oxidant for the remainder of the day.

Travnikov et al. [57] compared simulation results from four state-of-the-art chemical transport models with field data from various global and regional monitoring networks. It was found that models using the Br oxidation mechanism correctly simulated the observed seasonal variation of the  $\text{Hg}^{\text{II}}/\text{Hg}^0$  ratio in the near-surface layer but failed to predict the observed wet deposition maximum in summer at monitoring sites in North America and Europe. Models applying OH chemistry successfully predicted both the observed amplitude of seasonal changes and the periods of maximum and minimum values, but did not catch the maximum  $\text{Hg}^{\text{II}}/\text{Hg}^0$  ratios observed in spring. Models using  $\text{O}_3$  chemistry could not predict the observed large seasonal variation of either Hg oxidation or wet deposition flux.

Gencarelli et al. [68] simulated the deposition, transport and chemical interactions of atmospheric Hg over Europe for the year of 2013. The outputs of 14 model sensitivity tests were compared with field data from 28 monitoring sites. In general, good agreement was achieved between the model results and the observations. However, the observed deposition in precipitation was significantly underestimated when employing either the  $\text{O}_3$  or OH reaction mechanism alone. Using the Br oxidation mechanism overestimated  $\text{Hg}^{\text{II}}$  at the ground level and produced a lower overall Hg wet deposition than the simulations using both  $\text{O}_3$  and OH as atmospheric oxidants for  $\text{Hg}^0$ . These model results revealed that the field data could not be reproduced using the oxidation of  $\text{Hg}^0$  by  $\text{O}_3$ , OH or Br alone, which indicated a more complicated oxidation mechanism of atmospheric Hg.

Bieser et al. [69] performed a model comparison study evaluating the impact of oxidation schemes and emissions on atmospheric mercury. The models under study successfully simulated the concentration distribution of total Hg and  $\text{Hg}^0$  in the troposphere. It was found that the agreement between the observed  $\text{Hg}^{\text{II}}$  patterns and the model results employing different chemistry schemes seemed to depend on altitude. Although models using the Br oxidation scheme well simulated high concentrations of  $\text{Hg}^{\text{II}}$  in the upper troposphere, models applying  $\text{O}_3$  and OH chemistry better estimated elevated concentrations in the lower troposphere. However, more studies are needed to confirm this conclusion due to the possible significant influence of model results by the physical and chemical parameters used in these models.

Recent model studies seem to suggest that multiple oxidants are likely involved in the oxidation of atmospheric  $\text{Hg}^0$  dependent on seasons and locations. However, whether Br,  $\text{O}_3/\text{OH}$  or multiple oxidants are the major oxidants of  $\text{Hg}^0$  in the global atmosphere is unclear. To address this important question, more studies on reducing the large uncertainties in rate constants, understanding the heterogeneous oxidation reactions of  $\text{Hg}^0$ , as well as improving the treatment of chemical mechanisms in atmospheric Hg models and the accuracy of mercury emission inventories are needed [8,18,48].

### 3. Chemical Redox Reactions of Hg in the Aqueous Phase

To date, the proposed chemical oxidation pathways in atmospheric droplets include the aqueous-phase oxidation of  $\text{Hg}^0$  by  $\text{O}_3$ , OH, chlorine ( $\text{HOCl}/\text{OCl}^-$ ) and bromine ( $\text{Br}_2/\text{HOBr}/\text{BrO}^-$ ). The proposed chemical reduction pathways of mercury in the aqueous phase relevant to environmental conditions include the reduction of  $\text{Hg}^{\text{II}}$  by sulfite, photo-reduction of  $\text{Hg}(\text{OH})_2$ , photo-reduction of  $\text{Hg}^{\text{II}}$  by  $\text{HO}_2$  and photo-reduction of  $\text{Hg}^{\text{II}}$ -dicarboxylic acid complexes. The obtained rate constants and proposed mechanisms for these reactions were summarized in Table 2. Recent advances include the aqueous photoreduction of  $\text{Hg}^{\text{II}}$ -organic complexes and the effects of environmental variables on the aqueous reduction of  $\text{Hg}^{\text{II}}$  by sulfite.

**Table 2.** Current accumulated knowledge on chemical redox pathways of Hg in the aqueous phase.

Reactant (s)	Rate Constants	T (K)	pH	Potential Mechanism	Reference
Identified Aqueous Reduction Pathways of Hg <sup>2+</sup>					
Hg <sup>2+</sup> + sulfite (aq)	0.6 s <sup>-1</sup>	299	3.0–4.84	HgSO <sub>3</sub> → Hg <sup>+</sup> + HSO <sub>3</sub> <sup>-</sup> <i>or</i> + Hg <sup>+</sup> Hg <sup>0</sup> + products	[70]
	0.0106 ± 0.0009 s <sup>-1</sup>	298	3	HgSO <sub>3</sub> + nH <sub>2</sub> O → [Hg(SO <sub>3</sub> ) · (H <sub>2</sub> O) <sub>n</sub> ] → Hg <sup>0</sup> + products	[71]
	0.013 ± 0.007 s <sup>-1</sup>	298	7	Same as above	[72]
	<10 <sup>-4</sup> s <sup>-1</sup>	299	3.0–4.84	Hg(SO <sub>3</sub> ) <sub>2</sub> <sup>2-</sup> → Hg <sup>0</sup> + products	[70]
Hg(OH) <sub>2</sub>	3 × 10 <sup>-7</sup> s <sup>-1</sup>	293	7	Hg(OH) <sub>2</sub> $\xrightarrow{h\nu}$ [Hg(OH) <sub>2</sub> *] → Hg(OH)• + •OH → Hg <sup>0</sup> + products	[73]
HgS <sub>2</sub> <sup>2-</sup>	~10 <sup>-7</sup> s <sup>-1</sup>	298		Not available	[73]
Hg <sup>2+</sup> + HO <sub>2</sub>	1.7 × 10 <sup>4</sup> M <sup>-1</sup> s <sup>-1</sup>	298		C <sub>2</sub> O <sub>4</sub> <sup>2-</sup> + 2O <sub>2</sub> $\xrightarrow{h\nu}$ 2O <sub>2</sub> <sup>•-</sup> + 2CO <sub>2</sub> O <sub>2</sub> <sup>•-</sup> + H <sup>+</sup> → HO <sub>2</sub> <sup>•</sup> HO <sub>2</sub> <sup>•</sup> + Hg <sup>2+</sup> → Hg <sup>+</sup> + O <sub>2</sub> + H <sup>+</sup> HO <sub>2</sub> <sup>•</sup> + Hg <sup>+</sup> → Hg <sup>0</sup> + O <sub>2</sub> + H <sup>+</sup> HO <sub>2</sub> <sup>•</sup> + HO <sub>2</sub> <sup>•</sup> → H <sub>2</sub> O <sub>2</sub> + O <sub>2</sub>	[74]
				Not available	Intramolecular 2e <sup>-</sup> transfer via Hg <sup>2+</sup> -oxalate complex
Hg <sup>2+</sup> + Dicarboxylic acids (C <sub>2</sub> –C <sub>4</sub> )	(1.2 ± 0.2) × 10 <sup>4</sup> M <sup>-1</sup> s <sup>-1</sup> (Oxalic) (4.9 ± 0.8) × 10 <sup>3</sup> M <sup>-1</sup> s <sup>-1</sup> (Malonic); (2.8 ± 0.5) × 10 <sup>3</sup> M <sup>-1</sup> s <sup>-1</sup> (Succinic)	296	3.0	Mainly intramolecular 2e <sup>-</sup> transfer via Hg <sup>2+</sup> -dicarboxylate complexes	[76]
Identified Aqueous Oxidation Pathways of Hg <sup>0</sup>					
Hg <sup>0</sup> + O <sub>3</sub>	(4.7 ± 2.2) × 10 <sup>7</sup> M <sup>-1</sup> s <sup>-1</sup>	298	4.5–9.5	Hg <sup>0</sup> + O <sub>3</sub> → HgO + OH <sup>-</sup> + O <sub>2</sub> HgO + H <sup>+</sup> → Hg <sup>2+</sup> + OH <sup>-</sup>	[77]
Hg <sup>0</sup> + •OH	2.0 × 10 <sup>9</sup> M <sup>-1</sup> s <sup>-1</sup>	298		Hg <sup>0</sup> + •OH → Hg <sup>+</sup> + OH <sup>-</sup> Hg <sup>+</sup> + •OH → Hg <sup>2+</sup> + OH <sup>-</sup>	[74]
	(2.4 ± 0.3) × 10 <sup>9</sup> M <sup>-1</sup> s <sup>-1</sup>	298		Hg <sup>0</sup> + •OH → •HgOH •HgOH + O <sub>2</sub> + H <sub>2</sub> O → Hg(OH) <sub>2</sub> + H <sup>+</sup> + O <sub>2</sub> <sup>•-</sup> •HgOH + •OH → Hg(OH) <sub>2</sub> 2•HgOH → Hg <sub>2</sub> (OH) <sub>2</sub> ⇌ Hg <sup>0</sup> + Hg(OH) <sub>2</sub>	[78]
	5.5 × 10 <sup>9</sup> M <sup>-1</sup> s <sup>-1</sup>			Not available	[79]
Hg <sup>0</sup> + aqueous bromine	0.28 ± 0.02 M <sup>-1</sup> s <sup>-1</sup>	294–296	2, 6.8, 11.7	HOBr + Hg <sup>0</sup> → Hg <sup>2+</sup> + Br <sup>-</sup> + OH <sup>-</sup>	[80]
	0.27 ± 0.04 M <sup>-1</sup> s <sup>-1</sup>			OBr <sup>-</sup> + Hg <sup>0</sup> $\xrightarrow{H^+}$ Hg <sup>2+</sup> + Br <sup>-</sup> + OH <sup>-</sup>	
	0.2 ± 0.03 M <sup>-1</sup> s <sup>-1</sup>			Hg <sup>0</sup> + Br <sub>2</sub> → Hg <sup>2+</sup> + 2Br <sup>-</sup>	
Hg <sup>0</sup> + HOCl/OCl <sup>-</sup>	(2.09 ± 0.06) × 10 <sup>6</sup> M <sup>-1</sup> s <sup>-1</sup>	Ambient		HOCl + Hg <sup>0</sup> → Hg <sup>2+</sup> + Cl <sup>-</sup> + OH <sup>-</sup>	[81]
	(1.99 ± 0.05) × 10 <sup>6</sup> M <sup>-1</sup> s <sup>-1</sup>			OCl <sup>-</sup> + Hg <sup>0</sup> $\xrightarrow{H^+}$ Hg <sup>2+</sup> + Cl <sup>-</sup> + OH <sup>-</sup>	

### 3.1. Field Evidence for the Reduction of $\text{Hg}^{\text{II}}$

The first field observation of the sunlight-induced reduction of  $\text{Hg}^{\text{II}}$  in the atmosphere was recently reported by Foy et al. [82]. In their study, concentrations of  $\text{Hg}^0$ ,  $\text{Hg}^{\text{II}}$  and  $\text{Hg}_{(\text{p})}$  were monitored hourly over four winter months in a remote, high-altitude location. This study site is absent of local anthropogenic sources, which is ideal for studying atmospheric Hg chemical transformations. The parameters of a chemical box model required to reproduce the observations were determined using an optimization algorithm. It was found that the presence of a photolytic reduction reaction previously observed in laboratory studies was needed in order to match the model results with the field observations. The results suggested that the reduction reaction needs to be included in atmospheric Hg models in order to improve simulations of mercury deposition in the atmosphere.

### 3.2. Photoreduction of $\text{Hg}^{\text{II}}$ -Organic Complexes

$\text{Hg}^{\text{II}}$  could form strong complexes with organic ligands such as reduced sulfur groups [74,83–85]. The photoreduction of  $\text{Hg}^{\text{II}}$  in the presence of dissolved organic matter (DOM) has been widely documented in various natural water systems [86–90] and may also occur in atmospheric droplets and organic aerosols (OA) [91]. Recent model studies by Horowitz et al. supported the occurrence of the reduction of  $\text{Hg}^{\text{II}}$ -organic complexes in the atmosphere. Horowitz et al. [91] incorporated the updated chemical mechanism for atmospheric Hg into the GEOS-Chem global model and found that the inclusion of aqueous-phase photoreduction of  $\text{Hg}^{\text{II}}$ -organic complexes reported by Si and Ariya [76] in GEOS-Chem models, was critical for reproducing the observations. The major  $\text{Hg}^{\text{II}}$  deposition to the global oceans and the relatively low observed wet deposition of Hg over rural China may be due to different reduction rates of  $\text{Hg}^{\text{II}}$  with organic aerosols at various geographic locations.

### 3.3. Direct Reduction of $\text{Hg}^{\text{II}}$ by Sulfite

The aqueous-phase reduction of  $\text{Hg}^{2+}$  with sulfite is believed to be a process relevant to atmospheric droplets. The first-order rate constant determined by van Loon and her co-workers [71] has been widely used in current atmospheric Hg models. The effects of pH (1–7), temperature (274–318 K) and  $\text{Hg}^{\text{II}}$  sources ( $\text{Hg}(\text{NO}_3)_2$  or  $\text{HgO}$ ) on the aqueous-phase reduction rate were recently examined by Feinberg et al. [72] to better understand this reduction pathway. The results showed that the reduction could occur in the pH range of 1–7. The activation parameters of the aqueous  $\text{HgO}$  reduction by sulfite at pH 1 and 3 with  $T = 274\text{--}318\text{ K}$ , was in good agreement with the previous study [71]. The reduction rate at pH = 7 decreased with increasing ionic strength, especially with  $\text{Hg}(\text{NO}_3)_2$ . No statistical difference was found between the reduction rate constants of  $\text{Hg}(\text{NO}_3)_2$  and  $\text{HgO}$ , which suggested that the reduction of  $\text{Hg}^{\text{II}}$  by sulfite may be independent of the  $\text{Hg}^{\text{II}}$  species in the aqueous phase. The results indicated the possible occurrence of this reduction reaction under various environmental conditions and, thus, the necessity of its universal inclusion in atmospheric Hg models.

## 4. Heterogeneous Redox Reactions of Hg

As shown in Figure 1b, gaseous mercury species can adsorb on atmospheric surfaces and then undergo desorption, dissolution to atmospheric droplets or surface-enhanced (photo)chemical reactions [48]. Despite the potential significant role of heterogeneous Hg reactions on atmospheric Hg chemistry and model simulations [37,92], scarce data is available on mercury reactions and equilibrium processes on atmospheric surfaces such as aerosols [48]. A systematic understanding of the surface chemistry of Hg is extremely difficult [48,93] due to the varying concentration, size distribution and composition of aerosols at different locations, times and meteorological conditions [94,95]. Nevertheless, several recent laboratory studies focus on understanding the complex heterogeneous reactions between atmospheric mercury and various aerosols. The major findings in these studies are summarized in Table 3.

**Table 3.** Current accumulated knowledge on heterogeneous chemical reactions of Hg in the atmosphere.

Reactants	Surfaces	Major Findings	References
Hg <sup>2+</sup> + organic acids	0.1 g/L iron oxides particles or 0.01 g/L ambient aerosols	<ul style="list-style-type: none"> <li>The presence of iron oxides or ambient aerosols enhanced the rate.</li> <li>Proposed Mechanism: <math>\text{Fe}^{3+} - \text{OH} \xrightarrow{+OA} \text{Fe}^{3+} - \text{OA} \xrightarrow{h\nu} \text{R}^{\bullet} \xrightarrow{+\text{Hg}^{2+}} \text{Hg}^0</math></li> </ul>	[96]
HgCl <sub>2</sub>	Synthetic NaCl aerosols	<ul style="list-style-type: none"> <li>Significant reduction of Hg<sup>II</sup> observed upon UV, visible or a simulated solar radiation.</li> <li>The presence of iron in synthetic NaCl aerosols inhibited the reduction rate.</li> </ul>	[97]
HgCl <sub>2</sub>	Coal fly ash or synthetic aerosols	<ul style="list-style-type: none"> <li>The average half-life was estimated to be 1.6 h under clear sky atmospheric conditions from the reduction rates on three diverse fly ash samples;</li> <li>The reduction rate on low sulfate/low carbon fly ash was the fastest of the fly ash samples under study.</li> <li>The reduction rates on synthetic aerosols of carbon black and levoglucosan were about the same as those on coal fly ashes;</li> <li>The presence of adipic acid in synthetic aerosols significantly increased the reduction rate.</li> <li>The soluble constituents of fly ash may be important for the reduction.</li> </ul>	[98]
Hg <sup>2+</sup> + sulfite	Fly ash	<ul style="list-style-type: none"> <li>The presence of Cumberland and Shawnee fly ash samples inhibited the reduction rate.</li> <li>The reduction was observed in Cumberland fly ash without sulfite, possibly due to the richness of sulfur in these fly ash samples.</li> </ul>	[72]
HgCl <sub>2</sub> , HgBr <sub>2</sub> , Hg(NO <sub>3</sub> ) <sub>2</sub> , HgSO <sub>4</sub>	Fe(110), NaCl(100) and NaCl(111) <sup>Na</sup>	<ul style="list-style-type: none"> <li>The reduction was highly favorable on Fe(110) and NaCl(111)<sup>Na</sup> surfaces.</li> <li>The desorption of reduced Hg required either no energy input on the NaCl(111)<sup>Na</sup> surfaces or ~0.5 eV of external energy on the Fe(110) surfaces.</li> <li>The reduction of many Hg<sup>II</sup> species may proceed on metallic Fe and NaCl surfaces.</li> </ul>	[99]

Recently, Feinberg et al. [72] performed the first investigation of the kinetics of heterogeneous  $\text{Hg}^{\text{II}}$  reduction by sulfite ( $\text{Na}_2\text{SO}_3$ ) in the presence of fly ash using UV absorption spectroscopy. Compared with the corresponding homogeneous reduction rates of  $\text{Hg}^{\text{II}}$  by sulfite, the addition of fly ash samples from Cumberland Power Plant (Tennessee, USA) and Shawnee Fossil Plant (Kentucky, USA) reduced the reduction rates by c.a.45% and 95%, respectively. The observation of the  $\text{Hg}^{\text{II}}$  reduction in presence of the fly ash samples from Cumberland Power Plant (Tennessee) without added  $\text{Na}_2\text{SO}_3$ , may be due to the richness of sulfite in these fly ash samples. The existence of a large proportion of nanoparticles in the fly ash samples suggested that there were adequate surfaces for heterogeneous chemical reactions to occur. These results indicated the need to incorporate heterogeneous Hg reduction reactions into various environmental models of mercury.

Previous laboratory studies showed that the heterogeneous reduction reaction of  $\text{Hg}^{\text{II}}$  could occur on iron and sodium chloride aerosol surfaces, which are important components of atmospheric aerosols [97]. Recently, theoretical calculations by Tacey et al. [99] supported the experimental results. In this study, theoretical calculations were performed for the heterogeneous reduction reactions of  $\text{HgCl}_2$ ,  $\text{HgBr}_2$ ,  $\text{Hg}(\text{NO}_3)_2$  and  $\text{HgSO}_4$  on clean Fe(110), NaCl(100) and NaCl(111)<sup>Na</sup> surfaces. Here, Fe(110) was the most thermodynamically stable and, thus, the most abundant surface on metallic iron aerosols. The NaCl(100) facet is composed of neutrally charged layers with both Na and Cl atoms exposed on the surface, while NaCl(111)<sup>Na</sup> surfaces are charged layers exposing only Na atoms. The results indicated that the heterogeneous reduction reaction that generates  $\text{Hg}^0$  is highly favorable on Fe(110) and NaCl(111)<sup>Na</sup> surfaces. The desorption of reduced Hg required either no energy input on the NaCl(111)<sup>Na</sup> surfaces or ~0.5 eV of external energy on the Fe(110) surfaces. The results suggested that many oxidized mercury species can be heterogeneously reduced on metallic Fe and NaCl surfaces and the photochemical reaction on the aerosol surfaces may be a necessary step to catalyze the reaction.

Kurien et al. [100] used various iron(oxyhydr)oxide ( $\gamma\text{-Fe}_2\text{O}_3$ ,  $\alpha\text{-FeOOH}$ ,  $\alpha\text{-Fe}_2\text{O}_3$  and  $\text{Fe}_3\text{O}_4$ ) nanoparticles as proxies for reactive components of mineral dust and determined the uptake coefficients for the heterogeneous reaction of  $\text{Hg}^0_{(\text{g})}$  on these nanoparticles. Upon irradiation ( $\lambda = 290\text{--}700\text{ nm}$ ), the  $\text{Hg}^0_{(\text{g})}$  uptake kinetics significantly increased on  $\gamma\text{-Fe}_2\text{O}_3$ ,  $\alpha\text{-FeOOH}$ ,  $\alpha\text{-Fe}_2\text{O}_3$  nanoparticles, but not on the  $\text{Fe}_3\text{O}_4$  surface at  $P = 760 \pm 5\text{ Torr}$  and  $T = 295 \pm 2\text{ K}$ . The effect of radiation on the uptake of  $\text{Hg}^0_{(\text{g})}$  by  $\alpha\text{-Fe}_2\text{O}_3$  was retarded by relative humidity. The variation in the uptake behavior of the iron(oxyhydr) oxides nanoparticles was due to their different band gaps. More studies are needed to improve our understanding of such reactions.

Such research presents the need for further studies of the heterogeneous chemistry of mercury, because elemental mercury and many types of oxidized mercury are likely adsorbed and undergo (photo)chemical reactions in the presence of abundant atmospheric surfaces, such as particles and clouds.

## 5. Future Research Directions

Despite research progress in the understanding of the atmospheric processes of Hg, there are still major knowledge gaps in laboratory, theoretical and modeling studies, as well as field measurement. These gaps include but are not limited to mercury chemical speciation in the field, better kinetic and laboratory studies under various environmental conditions, and more consistent and sophisticated theoretical and modeling integration. We herein focus on the future research needs implied in recent studies since 2015.

Despite the potential importance of the oxidation of  $\text{Hg}^0$  by  $\text{O}_3/\text{OH}$  in the atmosphere, large uncertainties exist in the current gas-phase reaction rate constants and more studies need to be carried out to reduce these uncertainties in the first place. More studies are needed to evaluate the contribution of heterogeneous processes to the obtained rate coefficients for the oxidation of  $\text{Hg}^0$  by  $\text{O}_3$  and/or OH, in order to fully understand the discrepancy between the consistent experimental values and theoretical studies. Secondly, recent theoretical studies indicated that the oxidation of  $\text{Hg}^0$  could be initiated by Br- or Cl-atoms and then the secondary oxidation of the  $\text{HgX}$  ( $X = \text{Br}$  or  $\text{Cl}$ ) intermediate

could be carried out by  $\text{NO}_2$ ,  $\text{HO}_2$ ,  $\text{ClO}$ , or  $\text{BrO}$ . More laboratory studies are welcome to confirm this oxidation mechanism. Future field work and model sensitivity studies will also provide valuable insights into the viability of these reactions in the atmosphere. Since several studies supported the possible significant role of Br in the oxidation of  $\text{Hg}^0$  in the atmosphere, more kinetic and mechanistic studies are required to reduce the discrepancy in the reported rate constants for the oxidation of  $\text{Hg}^0$  by halogen atoms.

Recent model studies seemed to suggest that multiple oxidants are likely involved in the oxidation of atmospheric  $\text{Hg}^0$  dependent on seasons and locations. However, whether Br,  $\text{O}_3/\text{OH}$  or multiple oxidants are the major oxidants of  $\text{Hg}^0$  in the global atmosphere is unclear. Accurate measurements of vertical tropospheric concentration profiles of the species involved, such as various atmospheric oxidants,  $\text{Hg}^0_{(\text{g})}$  as well as detailed chemical compositions of oxidized mercury using diverse techniques, are critical for verifying the significance of various oxidants in Hg removal in the atmosphere globally.

Recent field observations and model studies supported the occurrence of reduction reactions in the atmosphere. Furthermore, their results supported the hypothesis that the reduction of  $\text{Hg}^{\text{II}}$ -organic complexes may play an important role in atmospheric Hg cycling besides sulfite-mediated reduction and photo-reduction of  $\text{Hg}(\text{OH})_2$ . More kinetic and mechanistic studies of  $\text{Hg}^{\text{II}}$  reduction pathways under environmentally-relevant conditions are needed. A better understanding of the reduction of  $\text{Hg}^{\text{II}}$  by organic compounds will require studies on the possible reduction pathways as well as on the quantification of various organic compounds in atmospheric droplets and aerosols.

Another important knowledge gap is the understanding of the redox reactions of Hg on various environmental surfaces such as aerosol, water, ice, snow, soil, and vegetative surfaces [48]. Despite the experimental difficulties caused by the variability in the size and composition of aerosols, several recent studies using fly ash or model aerosols have provided valuable information on understanding heterogeneous reactions of Hg on aerosols. The measured reaction rates are likely important in the chemical transformation of mercury in the atmosphere and the incorporation of these recent laboratory data in future model studies is essential to reduce uncertainties in current atmospheric Hg models. Such endeavors will benefit from the identification and quantification of oxidized mercury compounds, which has been a major challenge in atmospheric Hg research. There are novel instruments including mercury mass spectrometry [101], which can be used to provide such information. Further complementary analytical innovations to accurately quantify mercury-containing compounds in the atmosphere and atmospheric interfaces are needed.

In the light of the Minamata convention, we encourage a more integrated multi-disciplinary approach to comprehend mercury transformation, dynamics, speciation and remediation. Such integration is required to translate sound science to sound policy and regulations.

**Author Contributions:** Both authors made significant contributions. In particular, L.S. wrote the manuscript and P.A.A. revised, commented, and edited it.

**Acknowledgments:** We would like to thank the editor and two anonymous reviewers for their comments. We would like to thank the Natural Sciences and Engineering Research Council of Canada (NSERC), Environment Canada [Clean Air Regulatory Agenda (CARA)] and Auburn University at Montgomery for financial support. Lin Si would like to thank Emma for help with references.

**Conflicts of Interest:** The authors declare no conflict of interest.

## References

1. Miretzky, P.; Cirelli, A.F. Hg(II) removal from water by chitosan and chitosan derivatives: A review. *J. Hazard. Mater.* **2009**, *167*, 10–23. [[CrossRef](#)] [[PubMed](#)]
2. UNEP. *Global Mercury Assessment 2013: Sources, Emissions, Releases, and Environmental Transport*; UNEP Chemicals Branch: Geneva, Switzerland, 2013.
3. Khalizov, A.F.; Viswanathan, B.; Larregaray, P.; Ariya, P.A. Theoretical Study on the Reactions of Hg with Halogens: Atmospheric Implications. *J. Phys. Chem. A* **2003**, *107*, 6360–6365. [[CrossRef](#)]

4. Ariya, P.A.; Amyot, M.; Dastoor, A.; Deeds, D.; Feinberg, A.; Kos, G.; Poulain, A.; Ryjkov, A.; Semeniuk, K.; Subir, M.; et al. Mercury Physicochemical and Biogeochemical Transformation in the Atmosphere and at Atmospheric Interfaces: A Review and Future Directions. *Chem. Rev.* **2015**, *115*, 3760–3802. [[CrossRef](#)] [[PubMed](#)]
5. Shah, V.; Jaeglé, L.; Gratz, L.E.; Ambrose, J.L.; Jaffe, D.A.; Selin, N.E.; Song, S.; Campos, T.L.; Flocke, F.M.; Reeves, M.; et al. Origin of oxidized mercury in the summertime free troposphere over the southeastern US. *Atmos. Chem. Phys.* **2016**, *16*, 1511–1530. [[CrossRef](#)]
6. Driscoll, C.T.; Mason, R.P.; Chan, H.M.; Jacob, D.J.; Pirrone, N. Mercury as a Global Pollutant: Sources, Pathways, and Effects. *Environ. Sci. Technol.* **2013**, *47*, 4967–4983. [[CrossRef](#)] [[PubMed](#)]
7. Bergan, T.; Gallardo, L.; Rodhe, H. Mercury in the global troposphere: A three dimensional model study. *Atmos. Environ.* **1999**, *33*, 1575–1585. [[CrossRef](#)]
8. Zhang, L.; Lyman, S.; Mao, H.; Lin, C.-J.; Gay, D.A.; Wang, S.; Gustin, M.S.; Feng, X.; Wania, F. A synthesis of research needs for improving the understanding of atmospheric mercury cycling. *Atmos. Chem. Phys.* **2017**, *17*, 9133–9144. [[CrossRef](#)]
9. Pacyna, J.M.; Travnikov, O.; Simone, F.D.; Hedgecock, I.M.; Sundseth, K.; Pacyna, E.G.; Steenhuisen, F.; Pirrone, N.; Munthe, J.; Kindbom, K. Current and future levels of mercury atmospheric pollution on a global scale. *Atmos. Chem. Phys.* **2016**, *16*, 12495–12511. [[CrossRef](#)]
10. Schroeder, W.; Munthe, J. Atmospheric mercury—An overview. *Atmos. Environ.* **1998**, *5*, 809–822. [[CrossRef](#)]
11. Ryaboshapko, A.; Bullock, R.; Ebinghaus, R.; Ilyin, I.; Lohman, K.; Munthe, J.; Peterson, G.; Seigneur, C.; Wangberg, I. Comparison of mercury chemistry models. *Atmos. Environ.* **2002**, *36*, 3881–3898. [[CrossRef](#)]
12. Fitzgerald, W.F.; Mason, R.P. Biogeochemical cycling of mercury in the marine environment. *Metal Ions Biol. Syst.* **1997**, *34*, 53–111.
13. Ariya, P.A.; Skov, H.; Grage, M.M.L.; Goodsite, E.M. Gaseous elemental mercury in the ambient atmosphere: Review of the application of theoretical calculations and experimental studies for determination of reaction coefficients and mechanisms with halogens and other reactants. *Adv. Quantum Chem.* **2008**, *55*, 43–55.
14. Lin, C.-J.; Singhasuk, P.; Pehkonen, S.O. Atmospheric Chemistry of Mercury. In *Environmental Chemistry and Toxicology of Mercury*; Liu, G., Cai, Y., O'Driscoll, N., Eds.; John Wiley & Sons, Inc.: Hoboken, NJ, USA, 2012; pp. 113–153.
15. Jaffe, D.; Strode, S. Sources, fate and transport of atmospheric mercury from Asia. *Environ. Chem.* **2008**, *5*, 121–126. [[CrossRef](#)]
16. Lin, C.-J.; Pehkonen, S.O. The chemistry of atmospheric mercury: A review. *Atmos. Environ.* **1999**, *33*, 2067–2079. [[CrossRef](#)]
17. Ariya, P.A.; Peterson, K.; Snider, G.; Amyot, M. Mercury Chemical Transformations in the Gas, Aqueous and Heterogeneous Phases: State-of-the-Art Science and Uncertainties. In *Mercury Fate and Transport in the Global Atmosphere*; Springer: Dordrecht, The Netherlands, 2009; pp. 459–501.
18. Subir, M.; Ariya, P.A.; Dastoor, A.P. A review of uncertainties in atmospheric modeling of mercury chemistry I. Uncertainties in existing kinetic parameters—Fundamental limitations and the importance of heterogeneous chemistry. *Atmos. Environ.* **2011**, *45*, 5664–5676. [[CrossRef](#)]
19. Ariya, P.A.; Khalizov, A.F.; Gidas, A. Reaction of Gaseous Mercury with Atomic and Molecular Halogens: Kinetics, Product Studies, and Atmospheric Implications. *J. Phys. Chem. A* **2002**, *106*, 7310–7320. [[CrossRef](#)]
20. Spicer, C.W.; Satola, J.; Abbgly, A.A.; Plastringe, R.A.; Cowen, K.A. Kinetics of Gas-Phase Elemental Mercury Reaction with Halogen Species, Ozone, and Nitrate Radical Under Atmospheric Conditions. In *Final Report to Florida Department of Environmental Protection*; Battelle: Columbus, OH, USA, 2002.
21. Goodsite, M.E.; Plane, J.M.C.; Skov, H. A theoretical study of the oxidation of Hg<sup>0</sup> to HgBr<sub>2</sub> in the troposphere. *Environ. Sci. Technol.* **2004**, *38*, 1772–1776. [[CrossRef](#)] [[PubMed](#)]
22. Donohoue, D.L.; Bauer, D.; Cossairt, B.; Hynes, A.J. Temperature and pressure dependent rate coefficients for the reaction of Hg with Br and the reaction of Br with Br: A pulsed laser photolysis-pulsed laser induced fluorescence study. *J. Phys. Chem. A* **2006**, *110*, 6623–6632. [[CrossRef](#)] [[PubMed](#)]
23. Shepler, B.C.; Balabanov, N.B.; Peterson, K.A. Hg+Br→HgBr recombination and collision induced dissociation dynamics. *J. Chem. Phys.* **2007**, *127*, 164–304. [[CrossRef](#)] [[PubMed](#)]
24. Sun, G.; Sommar, J.; Feng, X.; Lin, C.-J.; Ge, M.; Wang, W.; Yin, R.; Fu, X.; Shang, L. Mass-dependent and -independent fractionation of mercury isotope during gas-phase oxidation of elemental mercury vapor by atomic Cl and Br. *Environ. Sci. Technol.* **2016**, *50*, 9232–9241. [[CrossRef](#)] [[PubMed](#)]

25. Jiao, Y.; Dibble, T.S. First kinetic study of the atmospherically important reactions  $\text{BrHg} + \text{NO}_2$  and  $\text{BrHg} + \text{HOO}$ . *Phys. Chem. Chem. Phys.* **2017**, *19*, 1826–1838. [[CrossRef](#)] [[PubMed](#)]
26. Greig, G.; Gunning, H.E.; Strausz, O.P. Reactions of metal atoms. II. The combination of mercury and bromine atoms and the dimerization of  $\text{HgBr}$ . *J. Chem. Phys.* **1970**, *52*, 3684–3690. [[CrossRef](#)]
27. Horne, D.G.; Gosavi, R.; Strausz, O.P. Reactions of metal atoms: Combination of mercury and chlorine atoms and the dimerization of  $\text{HgCl}$ . *J. Chem. Phys.* **1968**, *48*, 4758–4764. [[CrossRef](#)]
28. Donohoue, D.L.; Bauer, D.; Hynes, A.J. Temperature and pressure dependent rate coefficients for the reaction of  $\text{Hg}$  with  $\text{Cl}$  and the reaction of  $\text{Cl}$  with  $\text{Cl}$ : A pulsed laser photolysis/pulsed laser induced fluorescence study. *J. Phys. Chem. A* **2005**, *109*, 7732–7741. [[CrossRef](#)] [[PubMed](#)]
29. Byun, Y.; Cho, M.; Namkung, W.; Lee, K.; Koh, D.J.; Shin, D.N. Insight into the unique oxidation chemistry of elemental mercury by chlorine-containing species: Experiment and simulation. *Environ. Sci. Technol.* **2010**, *44*, 1624–1629. [[CrossRef](#)] [[PubMed](#)]
30. Slemr, F.; Schuster, G.; Seiler, W. Distribution, speciation, and budget of atmospheric mercury. *J. Atmos. Chem.* **1985**, *3*, 407–434. [[CrossRef](#)]
31. P'yankov, V.A. O kinetike Reaktsii Parov Rtuti s Ozonom (Kinetics of the Reaction of Mercury Vapour with Ozone). *Zhurnal Obscej. Chem. Akatemijaneuk SSSR* **1949**, *19*, 224–229.
32. Schroeder, W.; Yarwood, G.; Niki, H. Transformation processes involving mercury species in the atmosphere—Results from a literature survey. *Water Air Soil Pollut.* **1991**, *56*, 653–666. [[CrossRef](#)]
33. Iverfeldt, A.A.; Lindqvist, O. Atmospheric oxidation of elemental mercury by ozone in the aqueous phase. *Atmos. Environ.* **1986**, *20*, 1567–1573. [[CrossRef](#)]
34. Hall, B. The gas-phase oxidation of elemental mercury by ozone. *Water Air Soil Pollut.* **1995**, *80*, 301–315. [[CrossRef](#)]
35. Pal, B.; Ariya, P.A. Studies of ozone initiated reactions of gaseous mercury: Kinetics, product studies, and atmospheric implications. *Phys. Chem. Chem. Phys.* **2004**, *6*, 572–579. [[CrossRef](#)]
36. Sumner, A.; Spicer, C.; Satola, J.; Mangaraj, R.; Cowen, K.; Landis, M.; Stevens, R.; Atkeson, T. Environmental chamber studies of mercury reactions in the atmosphere. In *Dynamics of Mercury Pollution on Regional and Global Scales*; Springer: New York, NY, USA, 2005; pp. 193–212.
37. Snider, G.; Raofie, F.; Ariya, P.A. Effects of relative humidity and  $\text{CO}(\text{g})$  on the  $\text{O}_3$ -initiated oxidation reaction of  $\text{Hg}^0(\text{g})$ : Kinetic & product studies. *Phys. Chem. Chem. Phys.* **2008**, *10*, 5616–5623. [[PubMed](#)]
38. Rutter, A.P.; Shakya, K.M.; Lehr, R.; Schauer, J.J.; Griffin, R.J. Oxidation of gaseous elemental mercury in the presence of secondary organic aerosols. *Atmos. Environ.* **2012**, *59*, 86–92. [[CrossRef](#)]
39. Sommar, J.; Hallquist, M.; Ljungstrom, E.; Lindqvist, O. On the gas phase reactions between volatile biogenic mercury species and the nitrate radical. *J. Atmos. Chem.* **1997**, *27*, 233–247. [[CrossRef](#)]
40. Miller, G.C.; Quashnick, J.; Hebert, V. Reaction rate of metallic mercury with hydroxyl radical in the gas phase. *Abstr. Paper Am. Chem. Soc.* **2001**, *221*, 16-AGRO.
41. Bauer, D.; D'Ottone, L.; Campuzano-Jost, P.; Hynes, A.J. Gas phase elemental mercury: A comparison of LIF detection techniques and study of the kinetics of reaction with the hydroxyl radical. *J. Photochem. Photobiol. A* **2003**, *157*, 247–256. [[CrossRef](#)]
42. Pal, B.; Ariya, P.A. Gas-phase HO center dot-initiated reactions of elemental mercury: Kinetics, product studies, and atmospheric implications. *Environ. Sci. Technol.* **2004**, *38*, 5555–5566. [[CrossRef](#)] [[PubMed](#)]
43. Raofie, F.; Snider, G.; Ariya, P.A. Reaction of gaseous mercury with molecular iodine, atomic iodine, and iodine oxide radicals—Kinetics, product studies, and atmospheric implications. *Can. J. Chem.* **2008**, *86*, 811–820. [[CrossRef](#)]
44. Raofie, F.; Ariya, P.A. Product Study of the Gas-Phase  $\text{BrO}$ -Initiated Oxidation of  $\text{Hg}^0$ : Evidence for Stable  $\text{Hg}^1+$  Compounds. *Environ. Sci. Technol.* **2004**, *38*, 4319–4326. [[CrossRef](#)] [[PubMed](#)]
45. Seigneur, C.; Wrobel, J.; Constantinou, E. A chemical kinetic mechanism for atmospheric inorganic mercury. *Environ. Sci. Technol.* **1994**, *28*, 1589–1597. [[CrossRef](#)] [[PubMed](#)]
46. Tokos, J.J.S.; Hall, B.; Calhoun, J.A.; Prestbo, E.M. Homogeneous gas-phase reaction of  $\text{Hg}^0$  with  $\text{H}_2\text{O}_2$ ,  $\text{O}_3$ ,  $\text{CH}_3\text{I}$ , and  $(\text{CH}_3)_2\text{S}$ : Implications for atmospheric Hg cycling. *Atmos. Environ.* **1998**, *32*, 823–827. [[CrossRef](#)]
47. Dibble, T.S.; Zelig, M.J.; Mao, H. Thermodynamics of reactions of  $\text{ClHg}$  and  $\text{BrHg}$  radicals with atmospherically abundant free radicals. *Atmos. Chem. Phys.* **2012**, *12*, 10271–10279. [[CrossRef](#)]
48. Subir, M.; Ariya, P.A.; Dastoor, A.P. A review of the sources of uncertainties in atmospheric mercury modeling II. Mercury surface and heterogeneous chemistry—A missing link. *Atmos. Environ.* **2012**, *46*, 1–10. [[CrossRef](#)]

49. Hynes, A.J.; Donohoue, D.L.; Goodsite, M.E.; Hedgecock, I.M. Our current understanding of major chemical and physical processes affecting mercury dynamics in the atmosphere and at the air-water/terrestrial interfaces. In *Mercury Fate and Transport in the Global Atmosphere*; Springer: New York, NY, USA, 2009; pp. 427–457.
50. Peleg, M.; Tas, E.; Obrist, D.; Matveev, V.; Moore, C.; Gabay, M.; Luria, M. Observational Evidence for Involvement of Nitrate Radicals in Nighttime Oxidation of Mercury. *Environ. Sci. Technol.* **2015**, *49*, 14008–14018. [[CrossRef](#)] [[PubMed](#)]
51. Bergan, T.; Rodhe, H. Oxidation of elemental mercury in the atmosphere; constraints imposed by global scale modelling. *J. Atmos. Chem.* **2001**, *40*, 191–212. [[CrossRef](#)]
52. Dastoor, A.P.; Larcoque, Y. Global circulation of atmospheric mercury: A modelling study. *Atmos. Environ.* **2004**, *38*, 147–161. [[CrossRef](#)]
53. Selin, N.E.; Javob, D.J.; Park, R.J.; Yantosca, R.M.; Strode, S.; Jaeglé, L.; Jaffe, D. Chemical cycling and deposition of atmospheric mercury: Global constraints from observations. *J. Geophys. Res. Atmos.* **2007**, *112*, D02308. [[CrossRef](#)]
54. Travnikov, O.; Ilyin, I. The EMEP/MSC-E Mercury Modeling System. In *Mercury Fate and Transport in the Global Atmosphere: Emissions, Measurements, and Models*; Pirrone, N., Mason, R.P., Eds.; Springer: New York, NY, USA, 2009; pp. 571–587.
55. De Simone, F.; Gencarelli, C.N.; Hedgecock, I.M.; Pirrone, N. Global atmospheric cycle of mercury: A model study on the impact of oxidation mechanisms. *Environ. Sci. Pollut. Res.* **2014**, *21*, 4110–4123. [[CrossRef](#)] [[PubMed](#)]
56. Gencarelli, C.N.; de Simone, F.; Hedgecock, I.M.; Sprovieri, F.; Pirrone, N. Development and Application of a Regional-Scale Atmospheric Mercury Model Based on WRF/Chem: A Mediterranean Area Investigation. *Environ. Sci. Pollut. Res.* **2014**, *21*, 4095–4109. [[CrossRef](#)] [[PubMed](#)]
57. Travnikov, O.; Angot, H.; Artaxo, P.; Bencardino, M.; Bieser, J.; D’Amore, F.; Dastoor, A.; Simone, F.D.; Diéguez, M.d.C.; Dommergue, A.; et al. Multi-model study of mercury dispersion in the atmosphere: Atmospheric processes and model evaluation. *Atmos. Chem. Phys.* **2017**, *17*, 5271–5295. [[CrossRef](#)]
58. Mason, R.P.; Sheu, G.R. Role of the ocean in the global mercury cycle. *Glob. Biogeochem. Cycle* **2002**, *16*, 1093. [[CrossRef](#)]
59. Hedgecock, I.M.; Pirrone, N. Chasing quicksilver: Modeling the atmospheric lifetime of Hg-(g)(0) in the marine boundary layer at various latitudes. *Environ. Sci. Technol.* **2004**, *38*, 69–76. [[CrossRef](#)] [[PubMed](#)]
60. Dastoor, A.P.; Davignon, D.; Theys, N.; van Roozendaal, M.; Steffen, A.; Ariya, P.A. Modeling dynamic exchange of gaseous elemental mercury at polar sunrise. *Environ. Sci. Technol.* **2008**, *42*, 5183–5188. [[CrossRef](#)] [[PubMed](#)]
61. Holmes, C.D.; Jacob, D.J.; Yang, X. Global lifetime of elemental mercury against oxidation by atomic bromine in the free troposphere. *Geophys. Res. Lett.* **2006**, *33*, L20808. [[CrossRef](#)]
62. Theys, N.; van Roozendaal, M.; Hendrick, F.; Yang, X.; de Smedt, I.; Richter, A.; Begoin, M.; Errera, Q.; Johnston, P.V.; Kreher, K.; et al. Global observations of tropospheric BrO columns using GOME-2 satellite data. *Atmos. Chem. Phys.* **2011**, *11*, 1791–1811. [[CrossRef](#)]
63. Wang, S.Y.; Schmidt, J.A.; Baidar, S.; Coburn, S.; Dix, B.; Koenig, T.K.; Apel, E.; Bowdalo, D.; Campos, T.L.; Eloranta, E.; et al. Active and widespread halogen chemistry in the tropical and subtropical free troposphere. *Proc. Natl. Acad. Sci. USA* **2015**, *112*, 9281–9286. [[CrossRef](#)] [[PubMed](#)]
64. Gratz, L.E.; Ambrose, J.L.; Jaffe, D.A.; Shah, V.; Jaegle, L.; Stutz, J.; Festa, J.; Spolaor, M.; Tsai, C.; Selin, N.E.; et al. Oxidation of mercury by bromine in the subtropical Pacific free troposphere. *Geophys. Res. Lett.* **2015**, *42*, 10494–10502. [[CrossRef](#)]
65. Finlayson-Pitts, B.J.; Pitts, J.N.J. *Chemistry of the Upper and Lower Atmosphere, Theory, Experiments, and Applications*; Academic Press: San Diego, CA, USA, 2000.
66. Gustin, M.S.; Amos, H.M.; Huang, J.; Miller, M.B.; Heidecorn, K. Measuring and modeling mercury in the atmosphere: A critical review. *Atmos. Chem. Phys.* **2015**, *15*, 5697–5713. [[CrossRef](#)]
67. Ye, Z.; Mao, H.; Lin, C.-J.; Kim, S.Y. Investigation of processes controlling summertime gaseous elemental mercury oxidation at midlatitudinal marine, coastal, and inland sites. *Atmos. Chem. Phys.* **2016**, *16*, 8461–8478. [[CrossRef](#)]

68. Gencarelli, C.N.; Bieser, J.; Carbone, F.; Simone, F.D.; Hedgecock, I.M.; Matthias, V.; Travnikov, O.; Yang, X.; Pirrone, N. Sensitivity model study of regional mercury dispersion in the atmosphere. *Atmos. Chem. Phys.* **2017**, *17*, 627–643. [[CrossRef](#)]
69. Bieser, J.; Slemr, F.; Ambrose, J.; Brenninkmeijer, C.; Brooks, S.; Dastoor, A.; Simone, F.D.; Ebinghaus, R.; Gencarelli, C.N.; Geyer, B.; et al. Multi-model study of mercury dispersion in the atmosphere: Vertical and interhemispheric distribution of mercury species. *Atmos. Chem. Phys.* **2017**, *17*, 6925–6955. [[CrossRef](#)]
70. Munthe, J.; Xiao, Z.F.; Lindqvist, O. The aqueous reduction of divalent mercury by sulfite. *Water Air Soil Pollut.* **1991**, *56*, 621–630. [[CrossRef](#)]
71. Van Loon, L.; Mader, E.; Scott, S.L. Reduction of the aqueous mercuric ion by sulfite: UV Spectrum of HgSO<sub>3</sub> and Its Intramolecular Redox Reaction. *J. Phys. Chem. A* **2000**, *104*, 1621–1626. [[CrossRef](#)]
72. Feinberg, A.I.; Kurien, U.; Ariya, P.A. The Kinetics of Aqueous Mercury(II) Reduction by Sulfite Over an Array of Environmental Conditions. *Water Air Soil Pollut.* **2015**, *226*, 1–12. [[CrossRef](#)]
73. Xiao, Z.F.; Munthe, J.; Stromberg, D.; Lindqvist, O. Photochemical behavior of inorganic mercury compounds in aqueous solution. In *Mercury as a Global Pollutant-Integration and Synthesis*; Watras, C.J., Huckabee, J.W., Eds.; Lewis Publishers: Boca Raton, USA, 1994; pp. 581–592.
74. Pehkonen, S.O.; Lin, C.-J. Aqueous photochemistry of divalent mercury with organic acids. *J. Air Waste Manag. Assoc.* **1998**, *48*, 144–150. [[CrossRef](#)] [[PubMed](#)]
75. Gardfeldt, K.; Jonsson, M. Is bimolecular reduction of Hg(II) complexes possible in aqueous systems of environmental importance. *J. Phys. Chem. A* **2003**, *107*, 4478–4482. [[CrossRef](#)]
76. Si, L.; Ariya, P.A. Reduction of oxidized mercury species by dicarboxylic acids (C<sub>2</sub>–C<sub>4</sub>): Kinetic and product studies. *Environ. Sci. Technol.* **2008**, *42*, 5150–5155. [[CrossRef](#)] [[PubMed](#)]
77. Munthe, J. Aqueous oxidation of elemental Hg by O<sub>3</sub>. *Atmos. Environ.* **1992**, *26*, 1461–1468. [[CrossRef](#)]
78. Gardfeldt, K.; Sommar, J.; Stromberg, D.; Feng, X. Oxidation of atomic mercury by hydroxyl radicals and photoinduced decomposition of methylmercury in the aqueous phase. *Atmos. Environ.* **2001**, *35*, 3039–3047. [[CrossRef](#)]
79. Hines, N.A.; Brezonik, P.L. Mercury dynamics in a small Northern Minnesota lake: Water to air exchange and photoreactions of mercury. *Mar. Chem.* **2004**, *90*, 137–149. [[CrossRef](#)]
80. Wang, Z.; Pehkonen, S.O. Oxidation of elemental mercury by aqueous bromine: Atmospheric implications. *Atmos. Environ.* **2004**, *38*, 3675–3688. [[CrossRef](#)]
81. Lin, C.-J.; Pehkonen, S.O. Oxidation of elemental mercury by aqueous chlorine (HOCl<sup>-</sup>/OCl<sup>-</sup>): Implication for tropospheric mercury chemistry. *J. Geophys. Res.* **1998**, *103*, 28093–28102. [[CrossRef](#)]
82. Foy, B.D.; Tong, Y.; Yin, X.; Zhang, W.; Kang, S.; Zhang, Q.; Zhang, G.; Wang, X.; Schauer, J.J. First field-based atmospheric observation of the reduction of reactive mercury driven by sunlight. *Atmos. Environ.* **2016**, *134*, 27–39. [[CrossRef](#)]
83. Haitzer, M.; Aiken, G.R.; Ryan, J.N. Binding of mercury(II) to dissolved organic matter: The role of the mercury-to-DOM concentration ratio. *Environ. Sci. Technol.* **2002**, *36*, 3564–3570. [[CrossRef](#)] [[PubMed](#)]
84. Ravichandran, M. Interactions between mercury and dissolved organic matter—A review. *Chemosphere* **2004**, *55*, 319–331. [[CrossRef](#)] [[PubMed](#)]
85. Zheng, W.; Hintelmann, H. Mercury isotope fractionation during photoreduction in natural water is controlled by its Hg-DOC ratio. *Geochim. Cosmochim. Acta* **2009**, *73*, 6704–6715. [[CrossRef](#)]
86. Amyot, M.; Mierle, G.; Lean, D.R.S.; McQueen, D.J. Sunlight-induced formation of dissolved gaseous mercury in lake waters. *Environ. Sci. Technol.* **1994**, *28*, 2366–2371. [[CrossRef](#)] [[PubMed](#)]
87. Xiao, Z.F.; Stromberg, D.; Lindqvist, O. Influence of humic substances on photolysis of divalent mercury in aqueous solution. *Water Air Soil Pollut.* **1995**, *80*, 789–798. [[CrossRef](#)]
88. O'Driscoll, N.J.; Siciliano, S.D.; Lean, D.R.S.; Amyot, M. Gross photoreduction kinetics of mercury in temperate freshwater lakes and rivers: Application to a general model of DGM dynamics. *Environ. Sci. Technol.* **2006**, *40*, 837–843. [[CrossRef](#)] [[PubMed](#)]
89. Whalin, L.; Mason, R. A new method for the investigation of mercury redox chemistry in natural waters utilizing deflatable Teflon (R) bags and additions of isotopically labeled mercury. *Anal. Chim. Acta* **2006**, *558*, 211–221. [[CrossRef](#)]
90. Si, L.; Ariya, P.A. Aqueous photoreduction of oxidized mercury species in presence of selected alkanethiols. *Chemosphere* **2011**, *84*, 1079–1084. [[CrossRef](#)] [[PubMed](#)]

91. Horowitz, H.M.; Jacob, D.J.; Zhang, Y.; Dibble, T.S.; Slemr, F.; Amos, H.M.; Schmidt, J.A.; Corbitt, E.S.; Marais, E.A.; Sunderland, E.M. A new mechanism for atmospheric mercury redox chemistry: Implications for the global mercury budget. *Atmos. Chem. Phys.* **2017**, *17*, 6353–6371. [[CrossRef](#)]
92. Si, L.; Ariya, P.A. Photochemical Reactions of Divalent Mercury with Thioglycolic Acid: Formation of Mercuric Sulfide Particles. *Chemosphere* **2015**, *119*, 467–472. [[CrossRef](#)] [[PubMed](#)]
93. Prather, K.A.; Hatch, C.D.; Grassian, V.H. Analysis of atmospheric aerosols. *Ann. Rev. Anal. Chem.* **2008**, *1*, 485–514. [[CrossRef](#)] [[PubMed](#)]
94. Finlayson-Pitts, B.J. Reactions at surfaces in the atmosphere: Integration of experiments and theory as necessary (but not necessarily sufficient) for prediction the physical chemistry of aerosols. *Phys. Chem. Chem. Phys.* **2009**, *11*, 7760–7779. [[CrossRef](#)] [[PubMed](#)]
95. Seinfeld, J.H.; Pandis, S.N. *Atmospheric Chemistry and Physics*, 2nd ed.; John Wiley & Sons, Inc.: Hoboken, NJ, USA, 2006.
96. Lin, C.-J.; Pehkonen, S.O. Aqueous free radical chemistry of mercury in the presence of iron oxides and ambient aerosol. *Atmos. Environ.* **1997**, *31*, 4125–4137. [[CrossRef](#)]
97. Tong, Y.; Eichhorst, T.; Olson, M.R.; McGinnis, J.E.; Turner, I.; Rutter, A.P.; Shafer, M.M.; Wanga, X.; Schauer, J.J. Atmospheric photolytic reduction of Hg(II) in dry aerosols. *Environ.Sci. Processes Impacts* **2013**, *15*, 1883–1888. [[CrossRef](#)] [[PubMed](#)]
98. Tong, Y.; Eichhorst, T.; Olson, M.R.; Rutter, A.P.; Shafer, M.M.; Wang, X.; Schauer, J.J. Comparison of heterogeneous photolytic reduction of Hg(II) in the coal fly ashes and synthetic aerosols. *Atmos. Res.* **2014**, *138*, 324–329. [[CrossRef](#)]
99. Tacey, S.A.; Xu, L.; Mavrikakis, M.; Schauer, J.J. Heterogeneous Reduction Pathways for Hg(II) Species on Dry Aerosols: A First-Principles Computational Study. *J. Phys. Chem. A* **2016**, *120*, 2106–2113. [[CrossRef](#)] [[PubMed](#)]
100. Kurien, U.; Hu, Z.; Lee, H.; Dastoor, A.P.; Ariya, P.A. Radiation Enhanced Uptake of Hg<sup>0</sup>(g) on Iron (Oxyhydr)Oxide Nanoparticles. *RSC Adv.* **2017**, *7*, 45010–45021. [[CrossRef](#)]
101. Deeds, D.; Ghoshdastidar, A.; Raofie, F.; Guerette, E.-A.; Tessier, A.; Ariya, P. Development of a Particle-Trap Preconcentration-Soft Ionization Mass Spectrometric Technique for the Quantification of mercury halides in air. *Anal. Chem.* **2015**, *87*, 5109–5116. [[CrossRef](#)] [[PubMed](#)]



© 2018 by the authors. Licensee MDPI, Basel, Switzerland. This article is an open access article distributed under the terms and conditions of the Creative Commons Attribution (CC BY) license (<http://creativecommons.org/licenses/by/4.0/>).